*Key Engineering Materials*
*ISSN: 1662-9795, Vol. 936, pp 83-92*

*Submitted: 2022-07-03*
*Revised: 2022-09-25*
*Accepted: 2022-09-26*
*Online: 2022-12-14*

# Dielectric, AC Conductivity, and Optical Characterizations of (PVA-PEG) Doped SrO Hybrid Nanocomposites

Safa Ahmed Jabbar[1,a], Sarah Mohammed Khalil[2,b], Ali Razzaq Abdulridha[1,c], Ehssan Al-Bermany[1,d], Karar Abdali [3,e]

[1]Dep. of Physics, College of Education for Pure Science, University of Babylon, Iraq.

[2]Medical Physics Department, AL-Mustaqbal University College, Babylon, Iraq.

[3]Ministry of Education, Iraq.

[a]s.ahmed@uobabylon.edu.iq, [b]sarah.mohammed.khalil@mustaqbal-college.edu.iq, [c]ali_rzzq@yahoo.com, [d]ehssan@itnet.uobabylon.edu.iq, [e]aaazezphys@gmail.com
Corresponding email author: ehssan@itnet.uobabylon.edu.iq

**Keywords**: SrO, dielectric, electrical conductivity, optical and electrical properties.

**Abstract**. Strontium Oxide (SrO) nanoparticles have a specific structure, and excellent optical, mechanical, and thermal properties, within direct bandgap semiconductors applications. SrO impact on the optical and electrical properties of newly (PVA-PEG/ SrO) nanocomposite were investigated. The electrical properties were measured at 100 Hz – 6 MHz frequencies. An increase in frequency caused a reduction in the dielectric loss (δ) and dielectric constant (ε). ε value revealed an improvement with an increased loading ratio of SrO. The optical properties of the (PVA-PEG/SrO) nanocomposite showed a reduction in the energy gap values. In contrast, the absorption, extinction coefficient, absorption coefficient, optical conductivity, refractive index, and dielectric constant (imaginary, real) increased with the increased concentration of SrO NPs.

## Introduction

Polymers are a crucial material class in people's lives because they have deficient concentrations regarding the free charge carriers and are therefore non-conductive [1]. In addition, polymers as electric materials have the disadvantage of being transparent to electromagnetic radiation and providing protection against electrostatic discharge when dealing with sensitive electronic devices [2]. To overcome such limitations. The polymers' electrical properties represent through the response to the applied electric field (the subject of polymers' electrical characteristics encompasses a wide variety of molecular phenomena) [3]. When exposed to an electric field, polymers behave differently than metals. Polarisation is a phenomenon presenting the polymers' molecules rotating in the applied electric field direction [4].

One of the effective ways of probing important information about the polymers' electrical response in nature is molecular dynamics [5]. The electrical properties related to the final product might improve by combining at least two polymers (as blends) [6]. On the other hand, the appearance of additional properties depends on the blend's miscibility [7]. Blending may have significant and often unexpected impacts on thermal stability that cannot predict solely based on relative proportions and component behavior [8]. Televisions, displays, cellular phones, LEDs, batteries, solar cells, sensors, electromagnetic shielding, actuators, and microelectronic devices use conductive polymers [9].

Polymer-based composites are another type of material [10]. Electronic ones emphasize low dielectric constant, low thermal expansions, high thermal conductivity, and electromagnetic interference protection effectiveness could come from involving the nanomaterials with blended polymer to form environment conductive materials [11,12]. Conductive nanocomposites utilized as fillers could be ambitious for different applications [13]. In addition, a composite material is used as a structural material. The structural composites emphasize high modulus and strength based on the electronic application [14,15].

SrO is one of the direct bandgap semiconductor nanofillers belongs the II-VI semiconductor compounds group that is widely studied [16–19]. It has interesting properties, for instance, electrochemical stability, considerable exciting binding energy up to (60 meV), nontoxic, low-temperature growth, high transparency, and radiation resistance [16]. Because of the unique

hierarchical morphology of SrO NPs, it is used to design various electro-optical devices such as doped semiconductors, gas sensors, dye-sensitized solar cells, transistors, batteries electrodes, and supercapacitors [16,20]. This investigation aims to impact SrO nanofillers on the optical and electrical properties of (PVA-PEG/SrO) nanocomposites.

## Experimental and Theoretical Part

### Materials

Polyvinyl alcohol (PVA) made in Merck, Germany, with (14000) molecular weight, polyethylene glycol (PEG), and strontium oxide (SrO) nanoparticles, materials were used in this investigation.

### Sample preparations

SrO nanoparticles were utilized as an additive and added to a blended polymer matrix (PVA-PEG) with various loading weight percentage values (0, 1, 2, and 3) wt%. The samples for (PVA-PEG) and the (PVA-PEG/SrO) nanocomposites were made with the casting approach to create a sample with 1.5 μm thickness.

### Characterizations

UV/1800/Shimadzu spectrophotometer was used to photometrical measure the spectra. The dielectric constant of (PVA-PEG-SrO) composites was assessed with the use of an LCR meter with a frequency (f) between (100 Hz - 6 MHz) at room temperature.

### Calculations

The capacitance (C) was evaluated using the equation below [21].

$$C = \acute{\varepsilon} - \varepsilon_{\circ} At \quad (1)$$

here, represents dielectric constant; t represents sample thickness, and $\varepsilon_{\circ}$ represents the value of the vacuum permittivity. Loss factor (D) was evaluated from equation (2).

$$D = \acute{\varepsilon}/\acute{\varepsilon} \quad (2)$$

This represents electrical energy' loss that was dissipated as heat in the insulator. In addition, specifying power factors is vital in electrical applications. Also, the dielectric constant might be evaluated based on the following equation.

$$\varepsilon = C_p/C_o \quad (3)$$

here: $C_o$ represents vacuum capacitor, and $C_p$ represents parallel capacitance. Also, dissipated power in an insulator has been specified via the presence of alternating potential as an alternating conductivity function.

$$\sigma_{A.C} = w\, \acute{\varepsilon}\, \varepsilon_o \quad (4)$$

here, $\acute{\varepsilon}$ denotes the dielectric loss, and w represents the angular frequency.

## Results and Discussion

Figure (1) shows the dielectric constant variations with frequency. The constant dielectric results exhibited a decrease in the dielectric constant with the increasing applied frequency. In contrast, the increase in frequency leads to a reduction in the space polarised. The dielectric constant's value is impacted via the mechanism of polarization. The dielectric constant value increases at low-frequency values because material molecules will be partially polarized [22]. The dielectric constant value increased with the contribution of an increase in the loading ratio of SrO in PVA-PEG/SrO nanocomposites, as shown in Figure 2. The increase in the dielectric constant's value is because the particles of SrO are connected to create a network inside the polymer mixture. The increase in the

dielectric constant value is related to the increasing the SrO contained in the nanocomposites. The results matched the ones in the literature [23].

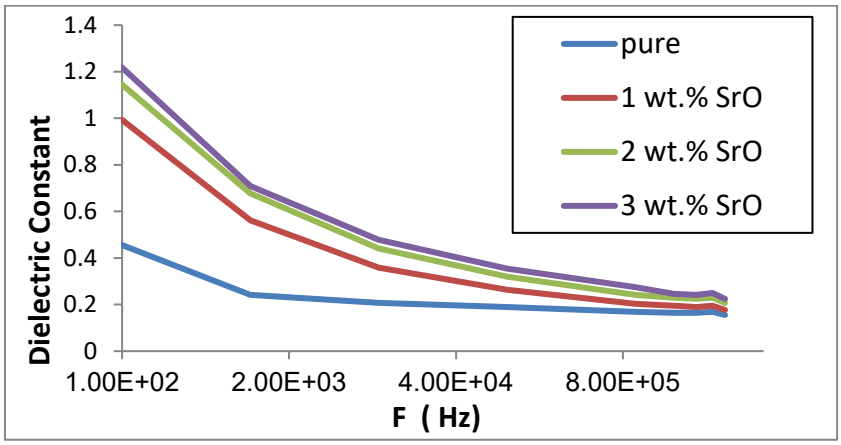


Figure 1: Effect of frequency on the dielectric constant of samples.

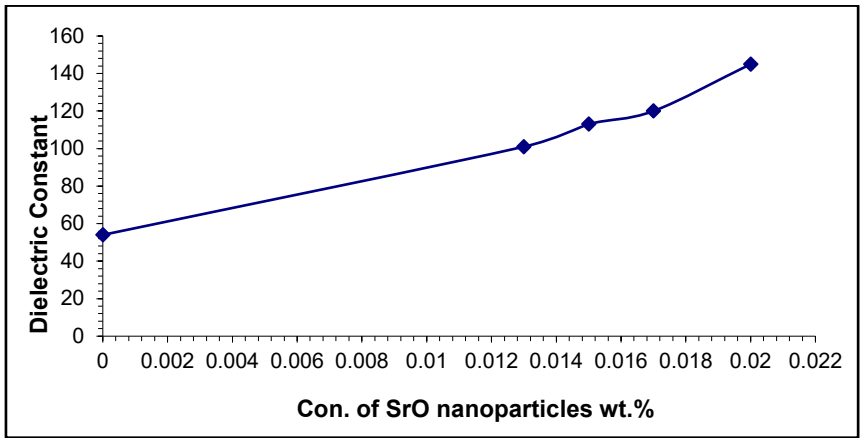


Figure 2: Effect of SrO concentrations on the dielectric constant of samples.

Figure 3 displays the relation between dielectric loss (δ) with frequency. The results indicate a reduction in the dielectric loss with increases in frequency. The results showed a high dielectric loss value at low frequency, decreasing with the frequency increase. This could be related to reducing the impact of the galaxy charge polarisation when the frequency was increased [24]. In addition, results showed improvement in the value of the dielectric loss with an increasing the SrO ratio in PVA-PEG/SrO nanocomposites; as shown in Figure 4, that trend might be related to an increase in dipole charge' alignments [25].

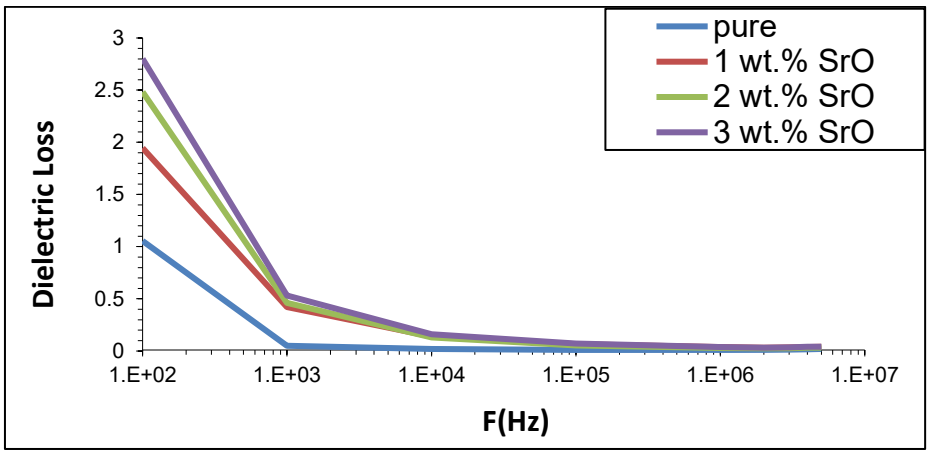


Figure 3: Effect of frequency on the level of the dielectric loss of samples.

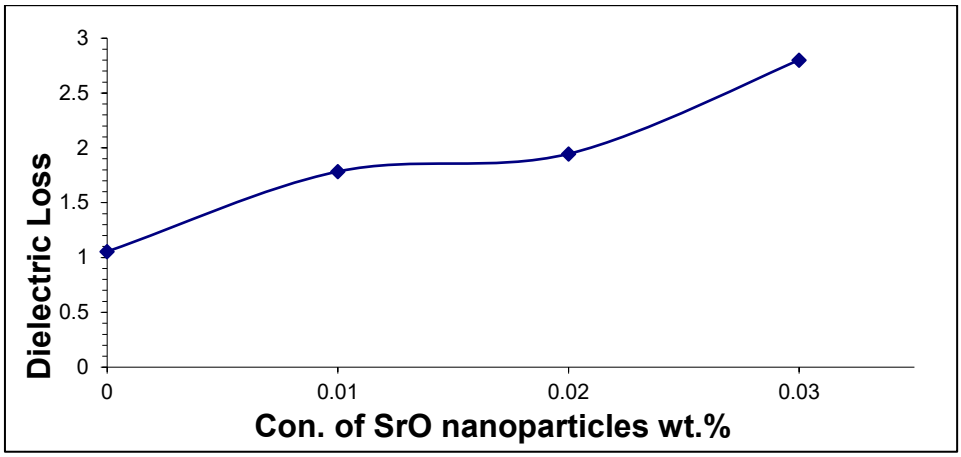


Figure 4: The effect of the Sb2O3 concentration on the dielectric loss of samples.

Figure.5 displays variations in electric conductivity results with frequency. This figure demonstrates enhancing the nanocomposites' conductivity with an increase in frequency, which might be due to space charge polarisation occurring at low-frequency values, along with charge carriers' motions, which move as in the hopping process. In conductivity, the increase was insignificant at high-frequency values, which might belong to electronic polarization and carriers of charge traveling via the hopping [15].

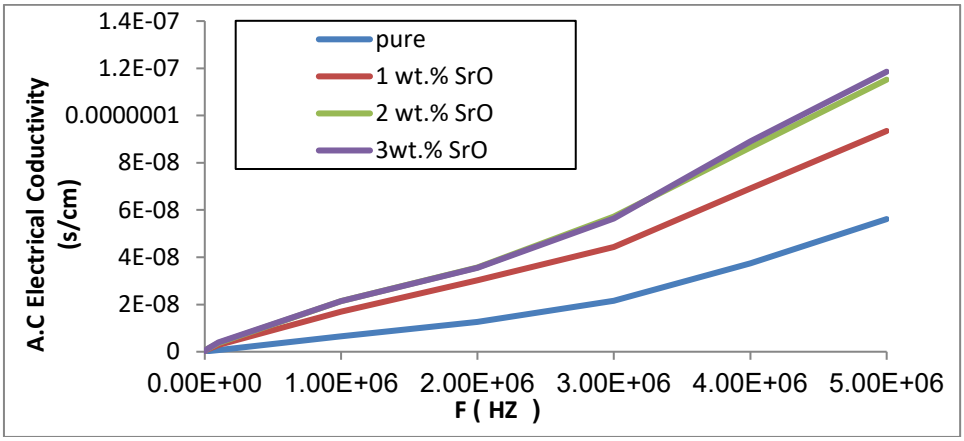


Figure 5; Effect of frequency on the electrical conductivity of samples.

The optical absorbance (A) behavior of blended polymers and nanocomposites was characterized by variable wavelengths in the range of (200-1100) nm at room temperature, as shown in Figure (6). Absorption spectra revealed a higher absorbance level in the UV range at 200 nm related to π-π*. Additional small peak features were presented at 280 nm that could be related to the nanofillers [26,27]. At high wavelengths, the incident photons do not have adequate energy for interacting with atoms and causing transmitting photons. However, all nanocomposites displayed low absorbance in the visible range; such behavior might be indicated in the following way, where the interactions between incident photon and material will occur. Thus, the increase in SrO NPs concentrations is associated with an increase in absorbance. Those results are comparable to the effects of researchers [28].

Figure (7) illustrates the transmittance spectra with a wavelength function of the samples. The transmittance decreased with increasing SrO nanoparticles concentrations that increased the adsorbed and attention the other light, as well as nanoparticles molecules, filled the most vacancies between (PVA-PEG) blends polymer [29].

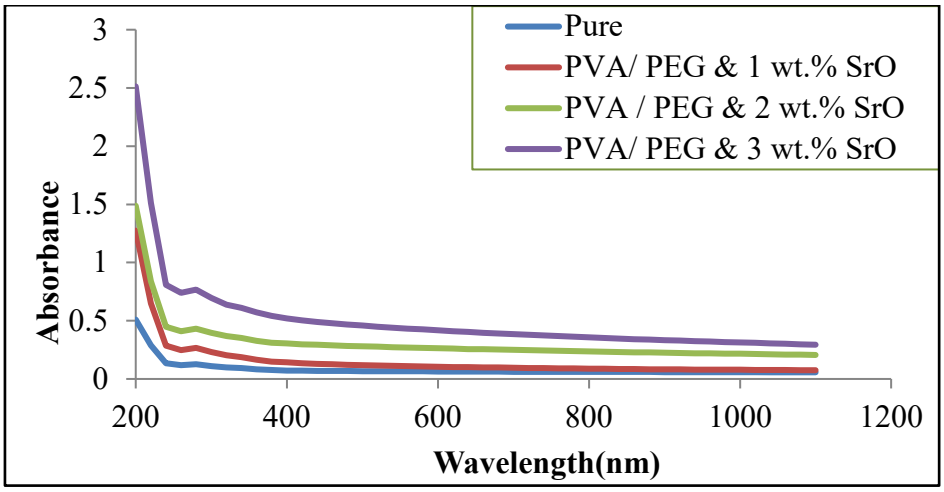


Figure 6: The absorbance as a wave-length function for the samples.

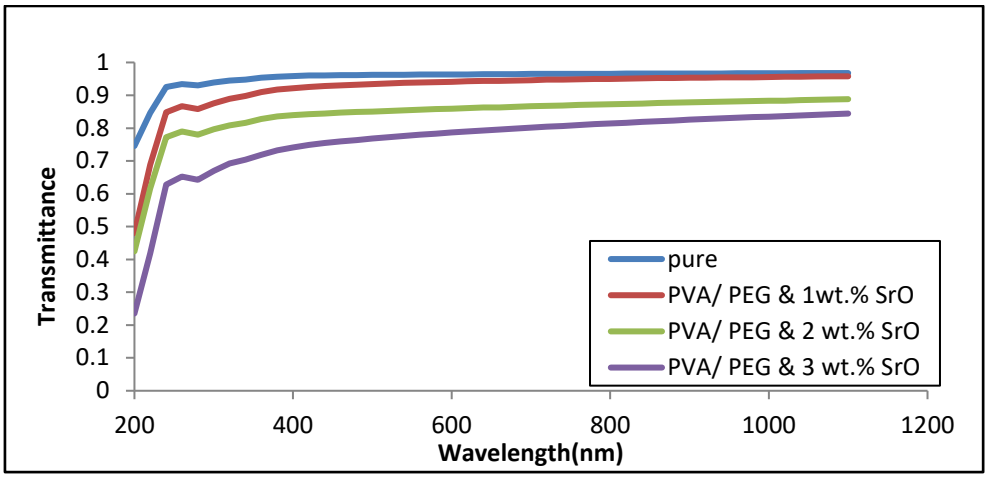


Figure 7: Transmittance with the wavelength for samples.

The absorption coefficient of the absorption α is computed using Eq. (5) [30].

$$\alpha = 2.3030 \frac{A}{t} \quad (5)$$

Here, A represents absorbance, and (t) represents the sample thickness.

Figure (8) illustrates the absorption coefficient (α) as a function of the samples' wavelength. The results showed small changes at the high wavelength (low energies), indicating the potential of low electronic transitions. At the low wavelength (high-energies), the absorption coefficient increased sharply, specifically at the photon's higher energy, indicating the significant probability that electronic transitions are the region's absorption edge [31]. Also, the absorption coefficient allows concluding the nature of the electronic transitions, where when the high absorption coefficient values (α is more than $10^4$ $cm^{-1}$) at high energies, direct electronic transitions are presented, and the energy and moment are maintained via photons and electrons [32].

The absorption coefficient values are low (α is less than $10^4$ $cm^{-1}$) at low energies where indirect electron transitions occur, while electronic momentum is maintained using a phonon [17]. The absorption coefficient values are low energies in the presented study, and indirect electronic transitions were deduced.

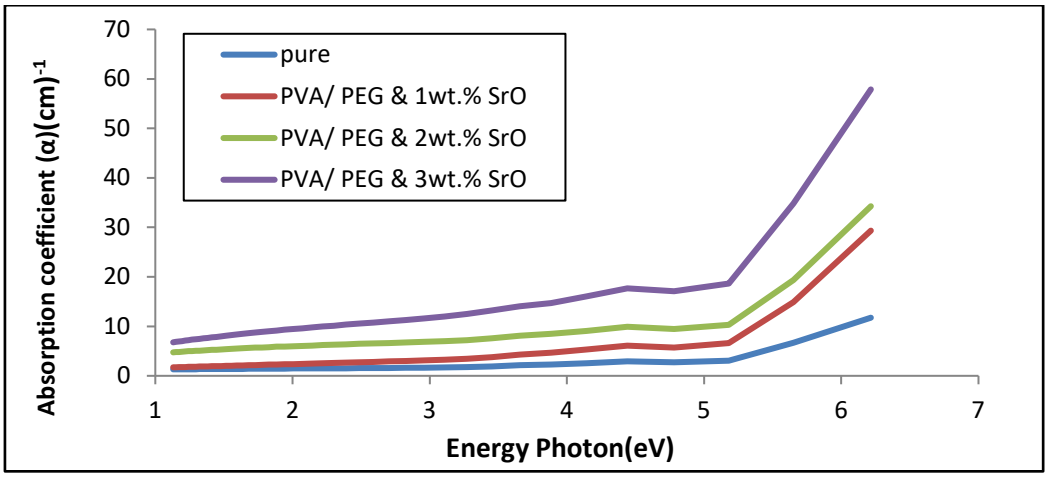


Figure 8: The absorption coefficient with energy photon of samples.

Figure (9) shows the relationship between $(\alpha h\nu)^{1/2}$ for samples with a photon energy function. On drawing a straight line from a curve's upper part towards the (x) axis, at a value of $(\alpha h\nu)^{1/2}=0$, the result is an energy gap for allowed indirect transitions. The values are listed in Table 1 using the Tauc relation [29].

$$(\alpha h\upsilon = B\ (\nu - E_g^{opt} \pm Eph)^{r} \quad (6)$$

It can be seen that the energy gap values were decreased by increasing the ratio of SrO NPs in the samples. This resulted in the on-site levels in the energy gap [33]. In this case, the transition is carried out in 2 stages, involving the electron transition from the band of valence to local conduction band levels due to the increase of SrO NPs. Such behavior results from electronic conduction's dependence upon the impurities that have been added [34]. The rise in SrO NP concentration levels provides electronic paths in blended polymer, facilitating the electron crossing from the valence to conduction bands. This explains the reduction in the energy gap with increasing the SrO NP concentrations [16]. The forbidden transitions of the indirect energy gap were computed similarly. Table (1) and Figures (9) note the energy gap for allowed and forbidden indirect transitions for samples.

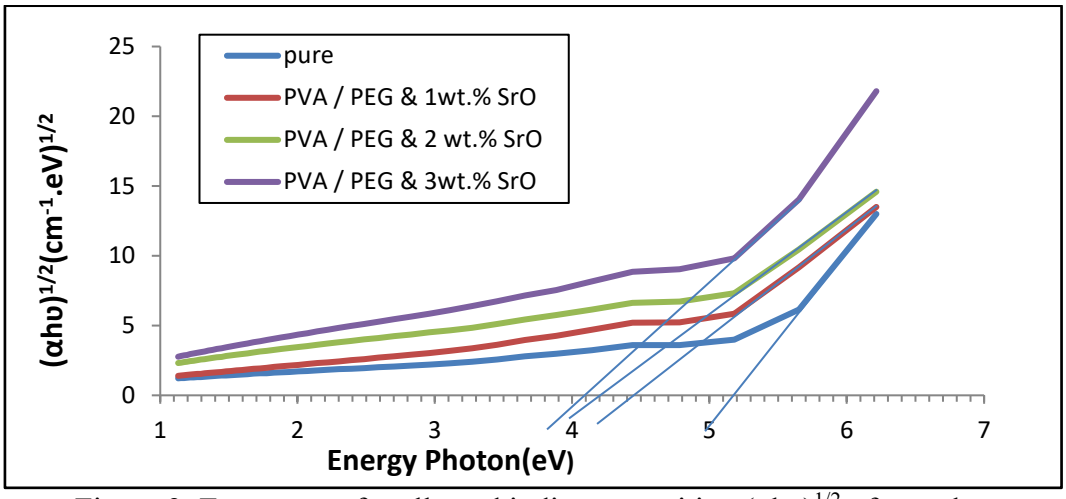


Figure 9: Energy gap for allowed indirect transition $(\alpha h\nu)^{1/2}$ of samples.

Table 1: Energy bandgap for allowed and forbidden indirect transitions for samples.

| SrO Nanoparticles concentrations | $E_g$ (eV) | |
|---|---|---|
| | **Allowed** | **Forbidden** |
| 0.00 | 5.15 | 4.9 |
| 0.01 | 4.45 | 3.95 |
| 0.02 | 4.2 | 3.6 |
| 0.03 | 4.1 | 3.4 |

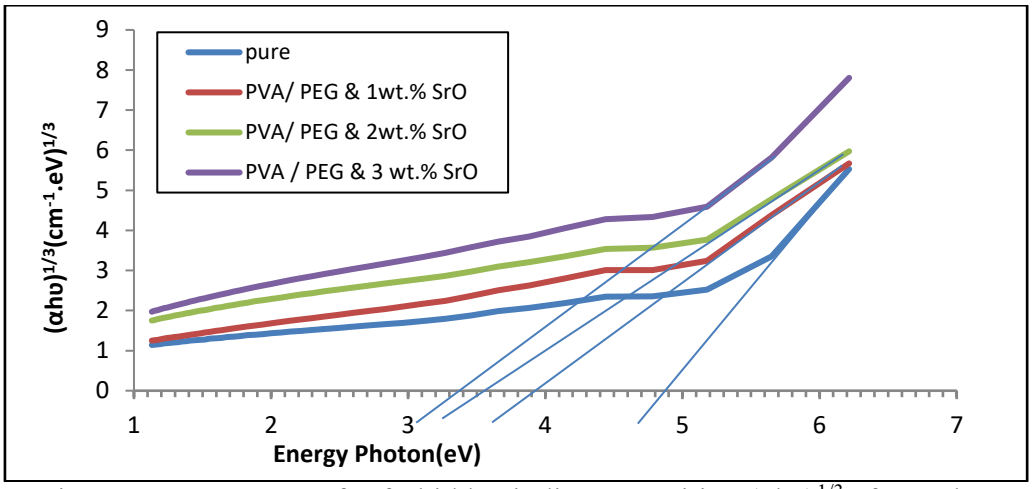


Figure 10: Energy gap for forbidden indirect transition $(\alpha h\upsilon)^{1/3}$ of samples.

Extinction coefficient (K) can be calculated according to eq (7) [25].

$$k = \alpha\lambda / 4\pi \tag{7}$$

The behavior of extinction coefficient (K) as a wavelength of samples is illustrated in Figure (11). (K) value was decreased with increasing the wavenumber slightly increased at the visible and the near IR region [35], which is why the extinction coefficient increased with the increase of the wavelength according to equation (6). The result of the absorption coefficient increased with the increasing the SrO nanoparticles concentrations [16,36], where it can conclude from equation (6) that the absorption coefficient is directly correlated to (K).

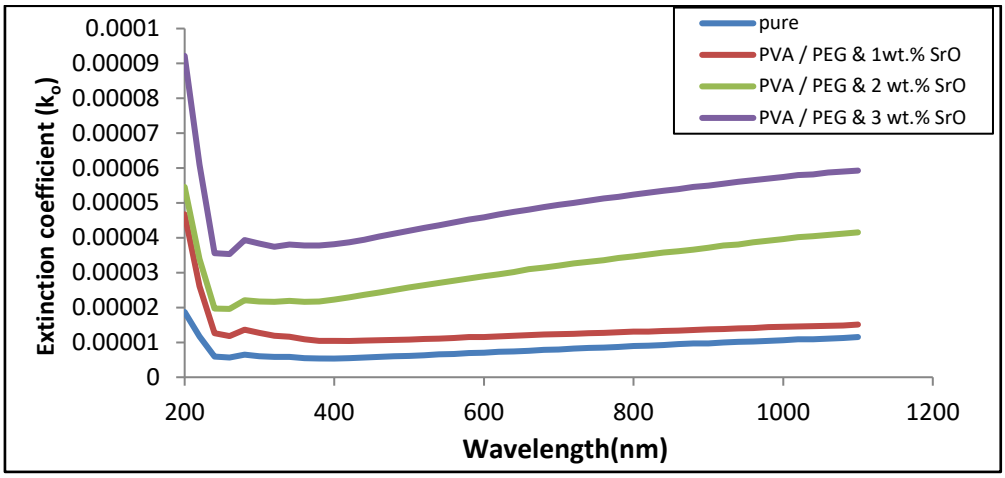


Figure 11: Coefficient of Extinction with the wavelengths for the samples.

The film's refractive index was estimated using equation (8) [37].

$$n = \frac{1+R}{1-R} + \left[\frac{4R}{(1-R)^2} - K_O{}^2\right]^{1/2} \tag{8}$$

The dispersion curves related to refractive index n, (λ) in the typical dispersion region (λ = 200- 1100 nm) are indicated in Figure (12) samples. Results illustrated a reduction in the values of (n) with the increase in wavelength and reached an almost constant value at the very long wavelength value [38]. Also, it was found that (n) was increased with the increased concentration ratio of SrO nanoparticles. The refractive index of (PVA-PVP) blends increased after embedding increasing SrO nanoparticles could result from the structural modifications in the polymeric matrix [17,39].

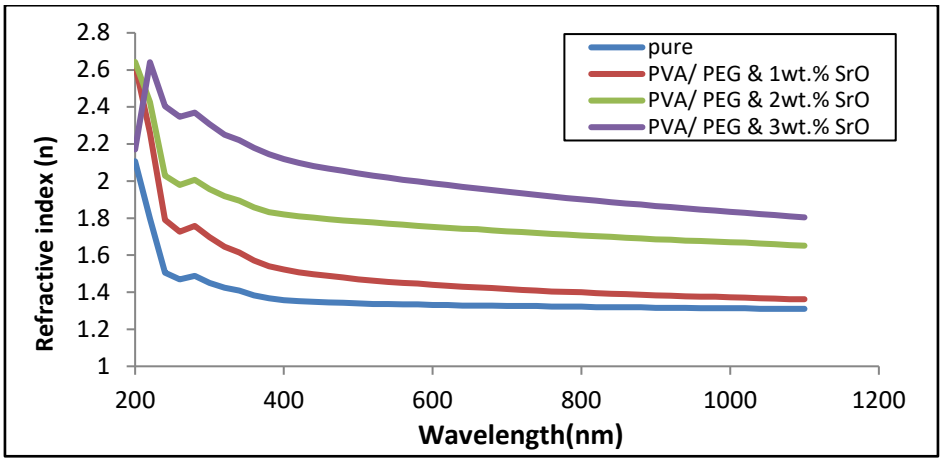


Figure 12: Refractive index with wavelength for samples

## Conclusions

The applied method successfully prepared PVA-PEG/SrO nanocomposite with different content of SrO. The contribution of SrO significantly improved the dielectric loss, dielectric constant, and electrical conductivity. Increasing the loading ratio of SrO and the applied electrical field' frequency enhances the electrical conductivity. The Absorbance at 200 nm increased from 0.51 to 2.51, and the energy gap improved from 5.15 to 4.1 eV for allowed from 4.9 to 3.4 eV of forbidden transactions after increasing the loading ratio of SrO NP. The absorption coefficient allows concluding the electronic transitions' nature when high absorption coefficient values ($\alpha > 10^4$) $cm^{-1}$ at high energies direct electronic transitions. The extinction coefficient also increased with the increase in wavelength. It is identified that there is an increase in (n) with the rise in SrO NPs concentrations. These results exhibited exiting nanocomposites promising for applications such as senses, solar cells, and elector-optical devices.

## References

[1] G.M. Joshi, K. Deshmukh, Electrical characterization of polymer composite gel under biasing as polar medium, Ionics. 20 (2014) 529–534.

[2] C.A. Grabowski, H. Koerner, J.S. Meth, A. Dang, C.M. Hui, K. Matyjaszewski, M.R. Bockstaller, M.F. Durstock, R.A. Vaia, Performance of Dielectric Nanocomposites: Matrix-Free, Hairy Nanoparticle Assemblies and Amorphous Polymer–Nanoparticle Blends, ACS Applied Materials & Interfaces. 6 (2014) 21500–21509.

[3] M. Abdul kadhim, E. Al-bermany, Enhance the Electrical Properties of the Novel Fabricated PMMA-PVA/ Graphene Based Nanocomposites, Journal of Green Engineering. 10 (2020) 3465–3483.

[4] K.L. Kim, W. Lee, S.K. Hwang, S.H. Joo, S.M. Cho, G. Song, S.H. Cho, B. Jeong, I. Hwang, J.-H. Ahn, Y.-J. Yu, T.J. Shin, S.K. Kwak, S.J. Kang, C. Park, Epitaxial Growth of Thin Ferroelectric Polymer Films on Graphene Layer for Fully Transparent and Flexible Nonvolatile Memory, Nano Letters. 16 (2016) 334–340.

[5] H. Lee, R.M. Venable, A.D. MacKerell, R.W. Pastor, Molecular Dynamics Studies of Polyethylene Oxide and Polyethylene Glycol: Hydrodynamic Radius and Shape Anisotropy, Biophysical Journal. 95 (2008) 1590–1599.

[6] C. Zhang, Q. Gao, B. Zhou, G. Bhargava, Preparation, characterization, and surface conductivity of nanocomposites with hollow graphitic carbon nanospheres as fillers in polymethylmethacrylate matrix, Journal of Nanoparticle Research. 19 (2017).

[7] E. Al-Bermany, B. Chen, Preparation and characterisation of poly(ethylene glycol)-adsorbed graphene oxide nanosheets, Polymer International. 70 (2021) 341–351.

[8] H. Wang, X. Liu, Z. Yang, H. He, X. Shao, R. Bai, Preparation and characterization of hexamethylenediamine-modified graphene oxide/Co-polyamide nanocomposites, Polymers and Polymer Composites. 28 (2020) 421–432.

[9] A. Harish Kumar, M.B. Ahamed, K. Deshmukh, M.S. Sirajuddeen, Morphology, Dielectric and EMI Shielding Characteristics of Graphene Nanoplatelets, Montmorillonite Nanoclay and Titanium Dioxide Nanoparticles Reinforced Polyvinylidenefluoride Nanocomposites, Journal of Inorganic and Organometallic Polymers and Materials. 31 (2021) 2003–2016.

[10] R. Krishnamoorti, R.A. Vaia, Polymer Nanocomposites, Journal of Polymer Science: Part B: Polymer Physics. 45 (2007) 3252–3256.

[11] X. Pei, Z. Zhu, Z. Gan, J. Chen, X. Zhang, X. Cheng, Q. Wan, J. Wang, PEGylated nano-graphene oxide as a nanocarrier for delivering mixed anticancer drugs to improve anticancer activity, Scientific Reports. 10 (2020) 2717, 1–15.

[12] A.K. Al-shammari, E. Al-Bermany, Polymer functional group impact on the thermo-mechanical properties of polyacrylic acid, polyacrylic amide- poly (vinyl alcohol) nanocomposites reinforced by graphene oxide nanosheets, Journal of Polymer Research. 29 (2022) 351.

[13] Y. Guo, X. Zuo, Y. Xue, J. Tang, M. Gouzman, Y. Fang, Y. Zhou, L. Wang, Y. Yu, M.H. Rafailovich, Engineering thermally and electrically conductive biodegradable polymer nanocomposites, Composites Part B: Engineering. 189 (2020) 107905.

[14] N.R. Glavin, R. Rao, V. Varshney, E. Bianco, A. Apte, A. Roy, E. Ringe, P.M. Ajayan, Emerging Applications of Elemental 2D Materials, Advanced Materials. 32 (2020) 1–22.

[15] S.S. Al-Abbas, R.A. Ghazi, A.K. Al-shammari, N.R. Aldulaimi, A.R. Abdulridha, S.H. Al-Nesrawy, E. Al-Bermany, Influence of the polymer molecular weights on the electrical properties of Poly(vinyl alcohol) – Poly(ethylene glycols)/Graphene oxide nanocomposites, Materials Today: Proceedings. 42 (2021) 2469–2474.

[16] S. Jayaraj, P. Vellaichamy, M. Sehar, A. Ramasamy, S.K. Ponnusamy, M.O. Daramola, Enhancement in thermal, mechanical and electrical properties of novel PVA nanocomposite embedded with SrO nanofillers and the analysis of its thermal degradation behavior by nonisothermal approach, Polymer Composites. 41 (2020) 1277–1290.

[17] V. Adimule, S.S. Nandi, B.C. Yallur, D. Bhowmik, A.H. Jagadeesha, Optical, Structural and Photoluminescence Properties of Gd x SrO: CdO Nanostructures Synthesized by Co Precipitation Method, Journal of Fluorescence. 31 (2021) 487–499.

[18] D.C. Sayle, J.A. Doig, S.A. Maicaneanu, G.W. Watson, Atomistic structure of oxide nanoparticles supported on an oxide substrate, Physical Review B - Condensed Matter and Materials Physics. 65 (2002) 1–15.

[19] T. Athar, Synthesis and Characterization of Strontium Oxide Nanoparticles via Wet Process, Materials Focus. 2 (2013) 450–453.

[20] R.A. Ghazi, K.H. Al-Mayalee, E. Al-Bermany, F.S. Hashim, A.K.J. Albermany, Impact of polymer molecular weights and graphene nanosheets on fabricated PVA-PEG/GO nanocomposites: Morphology, sorption behavior and shielding application, AIMS Materials Science. 9 (2022) 584–603.

[21] Y. Feng, X. Zhang, Y. Shen, K. Yoshino, W. Feng, A mechanically strong, flexible and conductive film based on bacterial cellulose/graphene nanocomposite, Carbohydrate Polymers. 87 (2012) 644–649.

[22] A.R. Kamali, D.J. Fray, Large-scale preparation of graphene by high temperature insertion of hydrogen into graphite, Nanoscale. 7 (2015) 11310–11320.

[23] M. Suresh, V. Siva, S.A. Bahadur, S. Athimoolam, Structural elucidation, hydrogen bonding motifs and solid state properties of p-toluenesulfonate salt of β-alaninine for optoelectronic device application, Journal of Molecular Structure. 1221 (2020) 128820.

[24] N.R. Aldulaimi, E. Al-Bermany, New Fabricated UHMWPEO-PVA Hybrid Nanocomposites Reinforced by GO Nanosheets: Structure and DC Electrical Behaviour, Journal of Physics: Conference Series. 1973 (2021) 012164.

[25] V.N. Suryawanshi, A.S. Varpe, M.D. Deshpande, Band gap engineering in PbO nanostructured thin films by Mn doping, Thin Solid Films. 645 (2018) 87–92.

[26] M.T. Hasan, B.J. Senger, C. Ryan, M. Culp, R. Gonzalez-Rodriguez, J.L. Coffer, A. V. Naumov, Optical Band Gap Alteration of Graphene Oxide via Ozone Treatment, Scientific Reports. 7 (2017) 6411.

[27] M.A. Kadhim, E. Al-Bermany, New fabricated PMMA-PVA/graphene oxide nanocomposites: Structure, optical properties and application, Journal of Composite Materials. 55 (2021) 2793–2806.

[28] F.J. Tommasini, L. da C. Ferreira, L.G.P. Tienne, V. de O. Aguiar, M.H.P. da Silva, L.F. da M. Rocha, M. de F.V. Marques, Poly (Methyl Methacrylate)-SiC Nanocomposites Prepared Through in Situ Polymerization, Materials Research. 21 (2018).

[29] J.I. Pankove, D.A. Kiewit, Optical Processes in Semiconductors, Journal of The Electrochemical Society. 119 (1972) 156C.

[30] A.I. Abdelamir, E. Al-Bermany, F. Sh Hashim, Enhance the Optical Properties of the Synthesis PEG/Graphene- Based Nanocomposite films using GO nanosheets, Journal of Physics: Conference Series. 1294 (2019) 022029.

[31] H. Liu, B. Zuo, Sound absorption property of PVA/PEO/GO nanofiber membrane and non-woven composite material, Journal of Industrial Textiles. 50 (2020) 512–525.

[32] S.B. Aziz, O.G. Abdullah, A.M. Hussein, R.T. Abdulwahid, M.A. Rasheed, H.M. Ahmed, S.W. Abdalqadir, A.R. Mohammed, Optical properties of pure and doped PVA:PEO based solid polymer blend electrolytes: two methods for band gap study, Journal of Materials Science: Materials in Electronics. 28 (2017) 7473–7479.

[33] N.R. Aldulaimi, E. Al-Bermany, Tuning the bandgap and absorption behaviour of the newly-fabricated Ultrahigh Molecular weight Polyethylene Oxide- Polyvinyl Alcohol/ Graphene Oxide hybrid nanocomposites, Polymers and Polymer Composites. 30 (2022) 096739112211121.

[34] A. Badawi, G.A.M. Mersal, A.A. Shaltout, J. Boman, M. Alsawat, M.A. Amin, Exploring the structural and optical properties of FeS filled graphene/PVA blend for environmental-friendly applications, Journal of Polymer Research. 28 (2021) 1–12.

[35] K. Kaviyarasu, D. Sajan, P.A. Devarajan, A rapid and versatile method for solvothermal synthesis of Sb2O3 nanocrystals under mild conditions, Applied Nanoscience (Switzerland). 3 (2013) 529–533.

[36] a F. Mansour, S.F. Mansour, M.A. Abdo, Improvement Structural and Optical Properties of ZnO/ PVA Nanocomposites, IOSR Journal of Applied Physics. 7 (2015) 60–69.

[37] C. Kittle, Introduction to Solid State Physics, 8th ed., John Wiley and Sons Inc., 2005.

[38] E.M. Abdelrazek, A.M. Abdelghany, S.I. Badr, M.A. Morsi, Structural, optical, morphological and thermal properties of PEO/PVP blend containing different concentrations of biosynthesized Au nanoparticles, Journal of Materials Research and Technology. 7 (2018) 419–431.

[39] A.K.H. Al-Khalaf, K. Abdali, A.O. Mousa, M.A. Zghair, Preparation and structural properties of liquid crystalline materials and its transition metals complexes, Asian Journal of Chemistry. 31 (2019) 393–395.